Compositional, Structural, and Optical Characterizations of $In_{1-X}Ga_xN$ Epilayers Grown by High Pressure Chemical Vapor Deposition

Ananta R. Acharya and Brian D. Thoms
Georgia State University, Department of Physics and Astronomy, Atlanta, GA 30303
Correspondence: aacharya@student.gsu.edu

Abstract

The compositional, structural and optical characterizations of $In_{1-x}Ga_xN$ epilayers grown by high pressure chemical vapor deposition have been carried out using Auger electron spectroscopy, x-ray diffraction and optical transmission spectroscopy. Auger electron spectroscopy revealed 14% gallium and 86% indium composition of the total metal contents in the $In_{1-x}Ga_xN$ epilayers. X-ray diffraction pattern showed three prominent peaks centered at 31.4°, 32.86° and 34.5° which are assigned to $In_{1-x}Ga_xN$ (0002), In (101) and GaN (0002) Bragg reflexes respectively. These results indicate no macroscopic observable phase separation in the analyzed $In_{1-x}Ga_xN$ sample. The optical transmission spectroscopy and the Beer-Lambert's law quatified the absorption band edge to be 1.6 eV for the analyzed $In_{1-x}Ga_xN$ epilayers.

Keywords: *$In_{1-x}Ga_xN$, AES, XRD, absorption band edge.*

Introduction

$In_{1-x}Ga_xN$, a ternary alloy system of two binaries GaN and InN, has received enormous attention due to its broad range of practical applications. This system has a direct band gap, high electron mobility, and high electron saturation velocity [1, 2]. Because of these outstanding properties, $In_{1-x}Ga_xN$ material has huge potential for optoelectronic devices such as high efficiency blue, green, and white light-emitting diodes [3], and laser diodes [4]. The optical band gap of $In_{1-x}Ga_xN$ alloy system can be tuned continuously from 0.7 eV (near-infra red) to 3.4 eV (ultraviolet), spanning almost over the whole solar spectrum [5] which offers a unique opportunity to design highly efficient multi-junction solar cells. Despite having remarkable physical properties and device applications, however, the growth of $In_{1-x}Ga_xN$ alloys and heterostructures has always been a difficult task. Difficulties associated with the growth of good quality $In_{1-x}Ga_xN$ are: (i) lower dissociation temperature of InN compared to that of GaN and (ii) large lattice mismatch (~11%) between the binaries InN and GaN. The large lattice mismatch may induce lattice strain [6] and contribute to a potential solid-phase miscibility gap in the ternary $In_{1-x}Ga_xN$ alloy system [7]. These factors may be a cause of the reported compositional inhomogeneity observed in $In_{1-x}Ga_xN$ epilayers [8-12], which reduces the device efficiencies of $In_{1-x}Ga_xN$ based optoelectronic structures. However, high pressure chemical vapor deposition has been found to be an effective technique to improve the phase stability in $In_{1-x}Ga_xN$ epilayers [13].

The structural properties of the $In_{1-x}Ga_xN$ epilayers play a significant role in determining the performance of the light emitting devices: for example, the output power and external efficiency of the laser diodes [14]. It is known that the crystalline microstructure quality is closely related to the growth parameters and hence they can affect the quality of the film considerably. It is reported that higher crystalline quality $In_{1-x}Ga_xN$ can be grown at high temperature (800 °C) but the amount of InN is low in the alloy. In contrast, higher InN content can be obtained at lower growth temperature (500 °C), but at the cost of crystalline quality [15]. The optical properties of $In_{1-x}Ga_xN$ are influenced by a number of factors: such as, growth rate, growth temperature,

thickness of $In_{1-x}Ga_xN$ and molar fraction of indium. In this paper, we have presented the structural, compositional and optical characterizations of $In_{1-x}Ga_xN$ epilayers using x-ray diffraction (XRD), Auger electron spectroscopy (AES) and optical transmission spectroscopy.

Experimental methods

The $In_{1-x}Ga_xN$ epilayers were grown at a reactor pressure of 15 bar, a nitrogen main carrier gas flow of 12 slm (standard liters per minute), a group V-III molar precursor ratio of 3000, and a group III composition set value of x = 0.15. The $In_{1-x}Ga_xN$ epilayers analyzed were grown by HPCVD on ~5 µm thick GaN/c-plane sapphire templates at 865 °C. Trimethylindium, Trimethylgallium and ammonia precursors were used to provide active indium, gallium and nitrogen fragments respectively to the growth surface. The precursors were provided to the growth surface via temporally controlled precursor pulses, which are embedded into the nitrogen main carrier gas stream.

For compositional analysis of $In_{1-x}Ga_xN$ epilayers, Auger electron spectroscopy was performed in a stainless-steel ultrahigh vacuum (UHV) system with a base pressure of 1.7×10^{-10} Torr. The details of the experimental set up, working principles and use of Auger electron spectroscopy have been published in previous papers [16, 17]. The sample was rinsed with isopropyl alcohol before insertion into the UHV chamber. Inside the UHV chamber, the sample was cleaned by a procedure of bombardment with 1 keV nitrogen ions followed by atomic hydrogen cleaning. The detail of the sample mount and cleaning procedures of sample inside the UHV chamber has been published elsewhere [18, 19].

XRD experiments were carried out utilizing an X`Pert PRO MPD (Philips) 4-circle diffractometer with a monochromatic x-ray (CuKα) source. XRD data were analyzed by Gaussian curve fitting to determine the position of Bragg reflexes.

In order to determine the absorption edge of $In_{1-x}Ga_xN$ epilayers, optical transmission experiment was carried out at room temperature using a UV-VIS-NIR (ultraviolet-visible-near infrared) spectrometer. The acquired optical transmission spectrum was corrected for detector, monochromator and light source characteristics and normalized to the growth template used. The optical absorption spectra of the epilayers were calculated from the optical transmission spectrum using Beer–Lambert's law in order to estimate the optical absorption edge of the $In_{1-x}Ga_xN$ alloy.

Results and discussion

The non-differentiated form of Auger electron spectrum from clean $In_{1-x}Ga_xN$ is depicted in Fig.1 (Ga peak observed at 1078 eV is not shown here). The peaks at 380 eV and 400 eV in the spectrum are assigned to nitrogen and indium peaks respectively. AES data can be represented in both differentiated and non differentiated forms. However, peak-to-peak heights in differentiated spectra cannot be used to find nitrogen to In ratios due to overlapping. Non-differentiated Auger electron spectra of InN and GaN are used for calibration to find composition of the $In_{1-x}Ga_xN$ film. The areas under nitrogen, indium and gallium peaks above the background are measured for InN, GaN and $In_{1-x}Ga_xN$. Ratios of the areas under indium to nitrogen and gallium to nitrogen peaks are measured for InN,

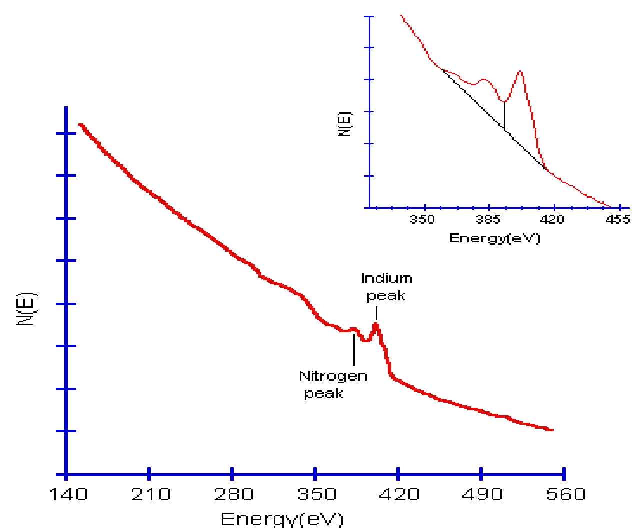

Fig. 1. Non-differentiated AES spectrum of HPCVD-grown $In_{1-x}Ga_xN$ sample (Ga peak has not been shown which is seen at 1078 eV) after sputtering followed by atomic hydrogen cleaning. Inset shows close view of Auger electron spectrum indicating areas under nitrogen and indium peaks above the background.

GaN and $In_{1-x}Ga_xN$. Dividing the ratio of gallium to nitrogen peak areas in $In_{1-x}Ga_xN$ spectrum by gallium to nitrogen peak areas in GaN spectrum, the Ga/N ratio is obtained for $In_{1-x}Ga_xN$. In the same way, In/N ratio is obtained for $In_{1-x}Ga_xN$ using the peak areas of InN and $In_{1-x}Ga_xN$ spectra. Once In/N and Ga/N are obtained, the fraction of In/Ga in $In_{1-x}Ga_xN$ is also calculated. Finally, fraction of each component is calculated taking the sum of fractions of Ga, In and nitrogen as unity. From this technique, we found 14% gallium and 86% indium out of total metal constituents in the analyzed sample. So, the composition on the analyzed $In_{1-x}Ga_xN$ sample is $In_{0.86}Ga_{0.14}N$. This is in excellent agreement with the set values of 15% gallium and 85% indium in the growth process as explained above in the experimental methods section.

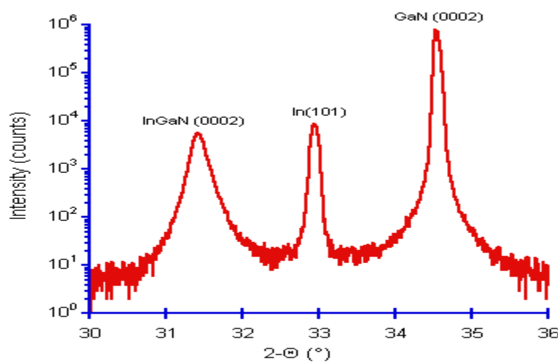

Fig. 2. XRD pattern of HPCVD-grown $In_{1-x}Ga_xN$ sample.

The x-ray diffraction pattern for the $In_{0.86}Ga_{0.14}N$ layers scanned in 2Θ-ω geometry is shown in Fig. 2. The XRD pattern shows three Bragg reflexes as shown in Fig. 2. The peak at 31.4° is assigned to $In_{1-x}Ga_xN$ (002) Brag relex. The peak observed at 32.86° is assigned to the residual metallic indium at the surface which is related to the In(101) Bragg reflex. The indium on the surface can be removed by 2 min wet etching in HCl after which the In(101) Bragg reflex at 32.86° is not observed anymore [19]. The peak centered at 34.5° is assigned to GaN (002) Bragg reflex related to the template on which the $In_{1-x}Ga_xN$ epilayers were grown. These results exhibit single $In_{1-x}Ga_xN$ (0002) Bragg reflex, indicating no macroscopic observable phase separation.

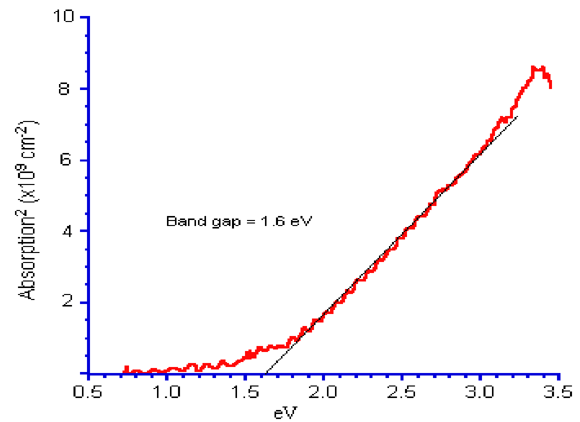

Fig. 3. Optical absorption spectrum of HPCVD-grown $In_{1-x}Ga_xN$.

The optical absorption spectra obtained for the $In_{1-x}Ga_xN$ epilayers is shown in Fig. 3. In order to estimate the optical absorption edge of the $In_{1-x}Ga_xN$ alloys, the optical transmission spectrum and Beer–Lambert's law have been employed. The Beer- Lambart's law in transmission spectroscopy is expressed as,

$$I_2 = I_1 \cdot e^{-\alpha(E) \cdot d} \quad (1)$$

where, I_2 and I_1 are the intensities of light through the substrate and the sample on the substrate respectively, α(E) is the absorption coefficient and d is the thickness of the sample. For direct semiconductor like $In_{1-x}Ga_xN$, $\alpha^2(E)$ can be linearly correlated with energy E. Graphing $\alpha^2(E)$ over spectral energy allows the estimation of the band gap value from the intercept of the slope of the $\alpha^2(E)$ line with the energy axis. Therefore, to quantify the absorption edge, a linear slope fit of the curve is used to obtain the intercept point with the energy axis. The optical absorption edge for the analyzed $In_{0.86}Ga_{0.14}N$ is found out to be 1.6 eV.

Conclusion

In summary, the compositional, structural and optical characterizations of $In_{1-x}Ga_xN$ grown by high pressure chemical vapor deposition were performed. For these characterizations, Auger electron spectroscopy, x-ray diffraction and optical transmission spectroscopy were employed. Auger electron spectroscopy revealed 14% gallium and 86% indium of the total metal

contents in the $In_{1-x}Ga_xN$ epilayers which were in close agreement with the set values of 15% gallium and 85% indium during the growth process. X-ray diffraction pattern confirmed the single phase $In_{1-x}Ga_xN$. Optical transmission spectroscopy showed the absorption band edge of 1.6 eV for the analyzed $In_{1-x}Ga_xN$ sample.

Acknowledgments
Authors would like to thank Dr. Dietz's research group in the department of Physics & Astronomy at Georgia State University for providing the sample and Dr. M. Jamil & Dr. I. Ferguson at Georgia Institute of Technology for providing the XRD data.

References

1. H. Morkoc, Nitride semiconductors and devices, Springer-Verlag, (1999).
2. Wu, J., W. Walukiewicz, K. M. Yu, W. Shan, J. W. Ager III, E. E. Haller, H. Lu, W. J. Schaff, W. K. Metzger, and S. Kurtz, J. of Appl. Phys. 94(10): 6477 6482. (2003).
3. S. Nakamura and G. Fasol, The Blue Laser Diode: GaN Based Light Emitters and Lasers (Springer, Berlin, 1997).
4. H. J. Choi, J. C. Johnson, R. He, S.-K. Lee, F. Kim, P. Pauzauskie, J. Goldberger, R. J. Saykally, and P. Yang, J. Phys. Chem. B 107, 8721 (2003).
5. J. Wu, W. Walukiewicz, K. M. Yu, J. W. Ager III, E. E. Haller, Hai Lu, and William J. Schaff, Appl. Phys. Lett. 80, 4741 (2002).
6. S. Yu. Karpov, MRS Internet J. Nitride Semicond. Res. 3, 16 (1998).
7. I. Ho, G.B. Stringfellow, Appl. Phys. Lett. 69, 2701-2703 (1996).
8. R. Singh, D. Doppalapudi, T. D. Moustakas, and L. T. Romano, Appl. Phys. Lett. 70, 1089 (1997).
9. B. N. Pantha, J. Li, J. Y. Lin, and H. X. Jiang, Appl. Phys. Lett. 93, 182107 (2008).
10. N. A. El-Masry, E. L. Piner, S. X. Liu, and S. M. Bedair, Appl. Phys. Lett. 72, 40 (1998).
11. C.A. Chang, C. F. Shin, N. C. Chen, T. Y. Lin, and K. S. Liu, Appl. Phys. Lett. 85, 6131 (2004).
12. K. Kushi, H. Sasamoto, D. Sugihara, S. Nakamura, A. Kikuchi and K. Kishino, Mater. Sci. Eng. B, 59 (1999).
13. G. Durkaya, M. Alevli, M. Buegler, R. Atalay, S. Gamage, M. Kaiser, R. Kirste, A. Hoffmann, M. Jamil, I. Fergusonand N. Dietz, Mater. Res. Soc. Symp. Proc. Vol. 1202 (2010).
14. F. K. Yam, Z. Hassan, Superlattices and Microstructures 43, 1-23 (2008).
15. G. Popovici, H. Morkoc, in: S. J. Pearton (Ed), GaN and Related Materials II, Gordon and Breach Science, Netherlands, p. 93 (2000).
16. A. R. Acharya, Himalayan Physics, Vol 1, 54 (2010).
17. A. R. Acharya and B. D. Thoms, Himalayan Physics, Vol 2, 35 (2011).
18. V. J. Bellitto, B. D. Thoms, D. D. Koleske, A. E. Wickenden, R. L. Henry, Surf. Sci. 430, 80 (1999).
19. A. R. Acharya, M. Buegler, R. Atalay, N. Dietz, J. S. Tweedie, R. Collazo and B. D. Thoms, J. Vac. Sci. Technol.A 29(4), 041402 (2011).